Tissue Eng Regen Med (2023) 20(7):1145–1159
https://doi.org/10.1007/s13770-023-00585-2

Online ISSN 2212-5469 TERM

ORIGINAL ARTICLE

circ_SPEF2 Regulates the Balance of Treg Cells by Regulating miR-16-5p/BACH2 in Lymphoma and Participates in the Immune Response

Jie Zhou[1] · Min Xu[1] · ZhaoZhao Chen[1] · LinLin Huang[1] · ZhuoLin Wu[1] · ZhongPei Huang[1] · Lin Liu[1]

Received: 5 June 2023 / Revised: 6 August 2023 / Accepted: 11 August 2023 / Published online: 6 October 2023

Abstract

BACKGROUND: This study aims to explore the potential mechanism of action of the newly discovered hsa_circ_0128899 (circSPEF2) in diffuse large B-cell lymphoma (DLBCL).

METHODS: circSPEF2, miR-16-5p and BTB and CNC homologue 2 (BACH2) expression patterns in DLBCL patients and cell lines were studied by RT-qPCR. The biological function of circSPEF2 *in vitro* and *in vivo* was investigated by function acquisition experiments. The proliferation activity of lymphoma cells was detected by MTT. Bax, Caspase-3, and Bcl-2 were determined by Western Blot. Apoptosis and the ratio of CD4 to Treg of immune cells in the co-culture system were analyzed by flow cytometry. The mechanism of action of circSPEF2 in DLBCL progression was further investigated by RIP and dual luciferase reporter experiments.

RESULTS: circSPEF2 was a circRNA with abnormally down-regulated expression in DLBCL. Increasing circSPEF2 expression inhibited the proliferative activity and induced apoptosis of lymphoma cells *in vitro* and *in vivo*, as well as increased $CD4^{+}$T cells and decreased Treg cell proportion of immune cells in the tumor microenvironment. Mechanically, circSPEF2 was bound to miR-16-5p expression, while BACH2 was targeted by miR-16-5p. circSPEF2 overexpression-mediated effects on lymphoma progression were reversible by upregulating miR-16-5p or downregulating BACH2.

CONCLUSIONS: circSPEF2 can influence DLBCL progression by managing cellular proliferation and apoptosis and the proportion of immune cells Treg and CD4 through the miR-16-5p/BACH2 axis.

Keywords circSPEF2 · miR-16-5p · BACH2 · Lymphoma

1 Introduction

Diffuse large B-cell lymphoma (DLBCL) is the most common type of lymphoma, accounting for about 30–40% of non-Hodgkin B-cell lymphoma [1]. DLBCL is a very aggressive malignancy, and its high heterogeneity and high rate of progression lead to unsatisfactory efficacy [2]. Therefore, it is urgent to find new targets and strategies to treat DLBCL and improve patients' life quality.

Immune escape refers to the phenomenon that tumor cells promote their own growth and metastasis by avoiding the recognition and attack of the immune system through various mechanisms, which is an important strategy for cancer proliferation, survival and development [3, 4]. The microenvironment of DLBCL has been reported to contain a large number of T cells, B cells, dendritic cells, and many cytokines [5]. Regulatory T cells are the most effective inhibitors of effector T cells and other immune cells, and have been accepted to inhibit the immune response of T cells to foreign and autoantigens [6]. In patients with lymphoma, the antitumor immune response may be

✉ Lin Liu
doctorliulin@hotmail.com

[1] Department of Hematology, Huazhong University of Science and Technology Tongji Medical College Affiliated Union Hospital, No. 1277 Jiefang Avenue, Jianghan District, Wuhan City 430022, Hubei Province, China

primarily mediated by T cells, which can induce apoptosis of cancer cells by killing their target cells through death receptor signaling or granulosa-dependent pathways [7, 8]. However, Tregs show immunosuppressive ability against T cells as well as B cells, monocytes, and dendritic cells [9–11]. Thus, the unbalanced proportion of immune cells in the tumor microenvironment (TME) is key to impaired tumor defense, which is closely related to lymphoma progression.

circRNA is a closed-loop ncRNA, mainly located in the cytoplasm, with high abundance, stability and characteristics associated with cancer progression, and is an ideal target for tumor diagnosis and treatment [12, 13]. circRNA has been increasingly recognized as a key regulatory factor in the pathological process of lymphoma [14–16]. Zhao et al. conducted circRNA high-throughput sequencing in DLBCL patients infected with EBV, and found that hsa_circ_012889 was abnormally downregulated [17]. hsa_circ_012889 is a SPEF2 gene derived from chromosome 5, with a length of 557 nt and named circSPEF2. However, no studies have reported the biological function of circSPEF2.

circRNAs can influence tumor progression through spongy miRNA or by regulating its target genes as a cancer promotion or tumor suppressor, respectively [18, 19]. miRNAs can regulate the expression of target genes at the post-transcriptional level, thus acting significantly in the process of cell differentiation, proliferation and apoptosis [20, 21]. Studies have confirmed that misexpressed miRNA is a key mechanism for the progression of DLBCL [22, 23]. It is worth noting that miR-16-5p has been proven to affect the malignant progression of a variety of tumors, such as osteosarcoma, breast cancer and non-small cell lung cancer [24–26]. However, miR-16-5p has been rarely studied in DLBCL.

BTB and CNC homologue 2 (BACH2) is a member of BTB-basic leucine zipper transcription factor family and is located on human chromosome 6 (6q15) [27]. BACH2, as a B-cell specific transcription factor, can regulate the shift-like recombination and somatic hypermutation of immunoglobulin genes. Previous studies have confirmed that BACH2 is highly expressed in T cells and B cells and is closely related to immune homeostasis [28–30].

This study explored the expression pattern of circSPEF2/miR-16-5p/BACH2 axis in DLBCL and defined their functions in DLBCL as well as related mechanisms in the immune response in the TME.

2 Materials and methods

2.1 Patients

The study was approved by the Medical Ethics Committee of Huazhong University of Science and Technology Tongji Medical College Affiliated Union Hospital (Approval number: C2016TJ1117). Dilated lymph node samples were harvested from 45 patients pathologically diagnosed with DLBCL, and corresponding tissue samples from 21 healthy donors were considered controls. Samples were collected before any anti-lymphoma therapy. Exclusion criteria: patients with other malignancies, autoimmune diseases and HIV/AIDS. Informed consent has been obtained for this study, and patient characteristics are listed in Table 1.

2.2 Cell culture

Human B lymphoma cell lines (SU-DHL-4 and U2932) and human normal lymphoblastic cell line (GM12878) were purchased from the BeNa culture bank (Suzhou, China). RPMI-1640 medium containing 10% fetal bovine serum (Gibco, Grand Island, NY, USA) and 1% penicillin/streptomycin (Invitrogen & Life Technologies, Carlsbad, CA, USA) was taken as the culture medium. The incubation conditions were set at 37 °C and 5% CO_2.

2.3 Cell transfection

oe-circSPEF2, miR-16-5p mimic, si-BACH2, and sh-BACH2, and their corresponding controls (Vector, mimic

Table 1 Primers

Genes	Sequences (5′–3′)
circSPEF2	Forward: AAAGCCAGCTTAGGAAATGCC
	Reverse: TCTTGCTTGTGATCCGGACG
miR-16-5p	Forward: CGGTAGCAGCACGTAAATA
	Reverse: GCAGGGTCCGAGGTATTC
BACH2	Forward: TCCACTGCACCAACATCCTC
	Reverse: CTGTGACCTCCTCAGGCAAG
U6	Forward: CTCGCTTCGGCAGCACA
	Reverse: AACGCTTCACGAATTTGCGT
GAPDH	Forward: CACCCACTCCTCCACCTTTG
	Reverse: CCACCACCCTGTTGCTGTAG

circSPEF2, circular RNA SPEF2; miR-16-5p, microRNA-16-5p; BACH2, BTB and CNC homology 1 basic leucine zipper transcription factor 2; GAPDH, glyceraldehyde-3-phosphatedehydrogenase

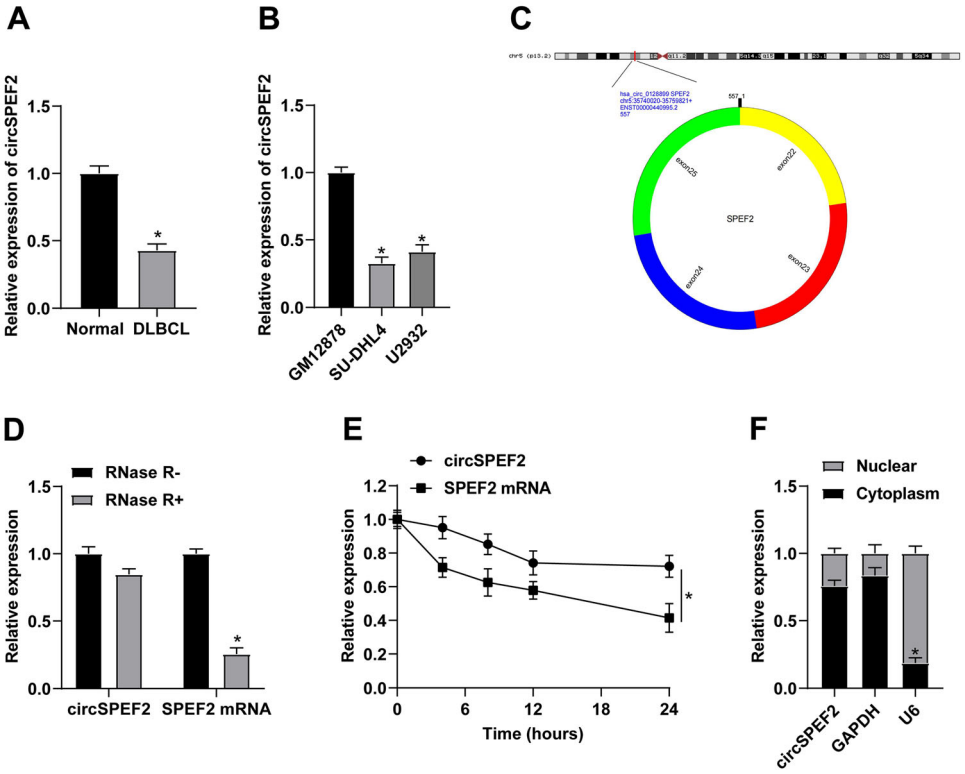

Fig. 1 Downregulated expression of circSPEF2 in DLBCL. **A**, **B** RT-qPCR checked circSPEF2 in DLBCL patients and controls and *in vitro* cell lines; **C** circSPEF2 structure diagram; **D**, **E** RNAse R and actinomycin D experiments verified the circSPEF2 ring structure; **F** The expression position of circSPEF2 in SU-DHL4 cells. Data were expressed as mean ± SD (N = 3). $p < 0.05$

NC, si-NC and sh-NC) were designed and synthesized from Genepharma (Shanghai, China), respectively. Moreover, the packaging and purification of sh-BACH2 lentivirus were completed by Genepharma. Detailed transfection procedures complied with Lipofectamine 3000 (Invitrogen) instructions. In short, SU-DHL-4 cells (3×10^5) were placed into a 6-well plate and replaced with a new medium at 6 h post-transfection, and cells were collected at 48 h post-transfection.

2.4 RNAse R assay

Total RNA from SU-DHL-4 was extracted, and 5 μg RNA was co-incubated with 2 U/g RNAse R (Epicentre Technologies, Chicago, IL, USA) at 37 °C for 30 min. Subsequently, the stability of circSPEF2 and circSPEF2 mRNA was detected by RT-qPCR.

2.5 Actinomycin D test

SU-DHL-4 cells (4×10^5) were treated with 2 μg/ml actinomycin D (MCE, HY-17559) and labeled at 0, 4, 8, 12, and 24 h. circSPEF2 and SPEF2 mRNA levels were analyzed by RT-qPCR.

2.6 Nucleo-plasmic separation

Nucleo-plasmic separation was performed using the PARIS™ kit (Life technologies, Carlsbad, CA, USA). SU-DHL-4 cells (1×10^6) were collected in the separation buffer, the nucleus and cytoplasm were separated by centrifugation, and total RNA was extracted respectively, followed by RT-qPCR to detect gene expression. U6 and GAPDH are the internal references of the nucleus and cytoplasm, respectively.

2.7 RT-qPCR

Total RNA was extracted from lymphoma tissues and cells using TRIzol® reagent (Invitrogen). The total RNA concentration and quality were measured by NanoDrop2000. To produce cDNA, reverse transcription was implemented using a cDNA synthesis kit (Thermo Fisher, Waltham, MA, USA). Then, RT-qPCR detection was conducted using SYBR Green Universal Master Mix reagent (Roche, Basel, Switzerland) or TaqMan microRNA assays (Thermo Fisher) for miRNA. The relative gene expression was calculated by $2^{-\Delta\Delta Ct}$. The primer sequence is shown in Table 1.

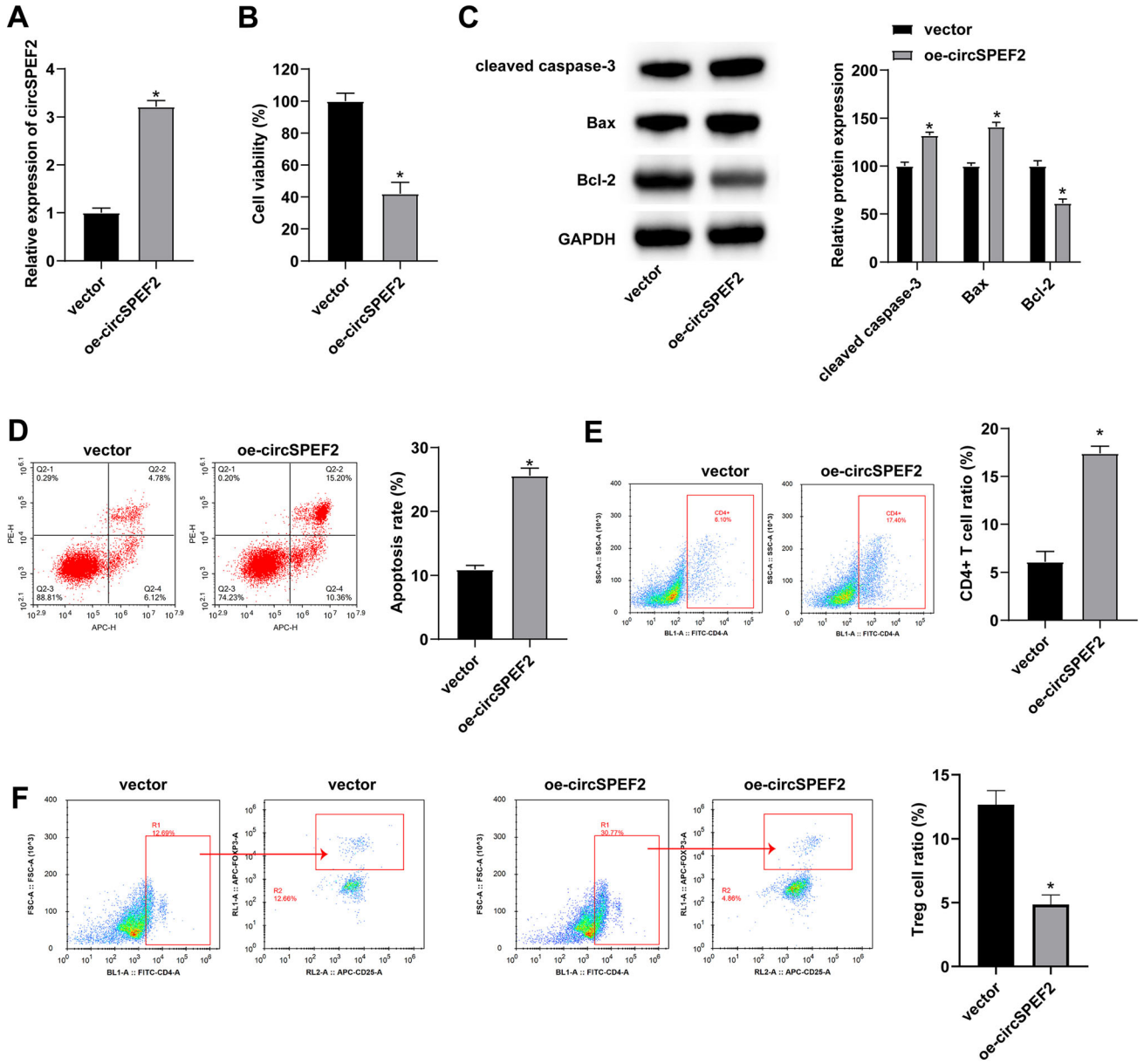

Fig. 2 circSPEF2 inhibits lymphoma cell proliferation and enhances the immune response. After transfection of oe-circSPEF2 in SU-DHL4 cells, **A** RT-qPCR checked circSPEF2 expression; **B** MTT assay analyzed the viability of SU-DHL4 cells; **C** Western blot measured apoptosis-related proteins; **D** Flow cytometry determined the apoptosis rate of SU-DHL4 cells in the co-culture system; **E**–**G** Flow cytometry detected the proportion of $CD4.^{+}$ and Treg cells in the co-culture system. Data were expressed as mean ± SD (N = 3). $p < 0.05$

2.8 Cell viability

SU-DHL-4 cells were inoculated in 96-well Petri dishes (5×10^3 cells/well) and mixed with 0% MTT solution (Guduo Biotechnology, Shanghai, China) at 48 h post-transfection. After 4 h, the supernatant was taken to incubate with 100 μL dimethyl sulfoxide (Sigma, Deisenhofen, Germany) for 10 min. Cell viability was measured at 490 nm with a microplate reader (Thermo Fisher).

2.9 Cell apoptosis

SU-DHL 4 cells were double-labeled with Annexin V FITC and PI solutions (Annexin V-FITC/PI Apoptosis

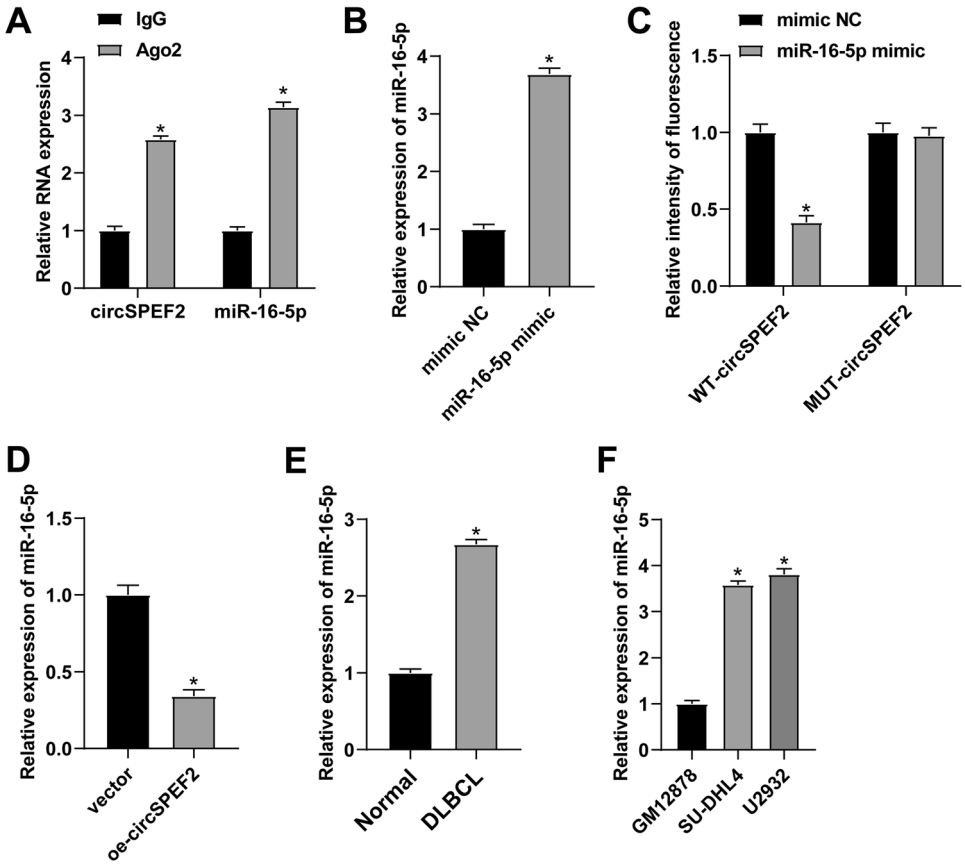

Fig. 3 miR-16-5p is targeted by circSPEF2. **A** Map of potential binding sites of circSPEF2 and miR-16-5p; **B** Ago2 enrichment level of circSPEF2 and miR-16-5p in SU-DHL4 cells; **C** RT-qPCR checked miR-16-5p; **D** Dual luciferase reporter assay verified the relationship between circSPEF2 and miR-16-5p; **E** After transfection of oe-circSPEF2 into SU-DHL4 cells, RT-qPCR checked miR-16-5p; **F**, **G** RT-qPCR checked miR-16-5p in tissues of DLBCL patients and cell lines. Data were expressed as mean ± SD (N = 3). $p < 0.05$

detection kit, Solarbio, Beijing, China, CA1020). Apoptosis rate was determined by flow cytometry. Apoptotic cells were Annexin V^+/PI^- and necrotic cells were Annexin V^+/PI^+.

2.10 Co-culture experiment

Human peripheral blood mononuclear cells (PBMCs) were isolated from peripheral blood of healthy volunteers and treated with 10% FBS, supplemented with 300 U/mL IL-2, human CD3 monoclonal antibody (10 μg/mL, 200 μL/well) and human CD28 monoclonal antibody (10 μg/mL, 200 μL/well) in RPMI-1640 medium for 72 h. SU-DHL-4 cells and T lymphocytes were cultured for 48 h. After staining with anti-CD3, anti-CD4, anti-CD25 and anti-Foxp3 antibodies, the proportions of $CD4^+$T cells and Treg cells were analyzed by flow cytometry. $CD3^+CD4^+$ were CD4 + T cells, and $CD4^+CD25^+Foxp3^+$ were Treg cells [31]. All the antibodies were purchased from BD Corporation (Bedford, MA, USA).

2.11 Western blot

Precooled RIPA cell lysis solution (Beyotime, Shanghai, China) was utilized to lysate the cells on ice for 30 min and protein concentrations were determined using a BCA kit (Pierce Biotechnology, Rockford, IL, USA). Protein samples were isolated on 10% SDS-PAGE and subsequently transferred to PVDF membranes (Thermo Fisher). After washing the membrane with TBST, it was blocked with 5% BSA and treated with anti-BACH2 (ab83364, 1:1000), anti-Bax (ab53154, 1:1,000), anti-Caspase-3 (Caspase-3, 1:1,000), anti-Bcl-2 (ab32124, 1:1,000) and GAPDH (ab8245, 1:1000) overnight at 4 °C. Then, the membrane was incubated with the corresponding secondary antibody (1:500) at room temperature for 1 h. All antibodies were purchased from Abcam (Cambridge, UK). Finally, the images were developed using the enhanced chemiluminescence kit (UltraSignal, Beijing, China).

2.12 RIP

RIP experiments were conducted using the Magna RIP kit (Millipore, Burlington, MA, USA). Cells were lysed with RIP lysis buffer solution, and the supernatant was mixed with an appropriate amount of magnetic beads binding to Ago2 or IgG antibody at 4 °C overnight. After elution, the immunoprecipitates were conditioned to RNA extraction for RT-qPCR analysis.

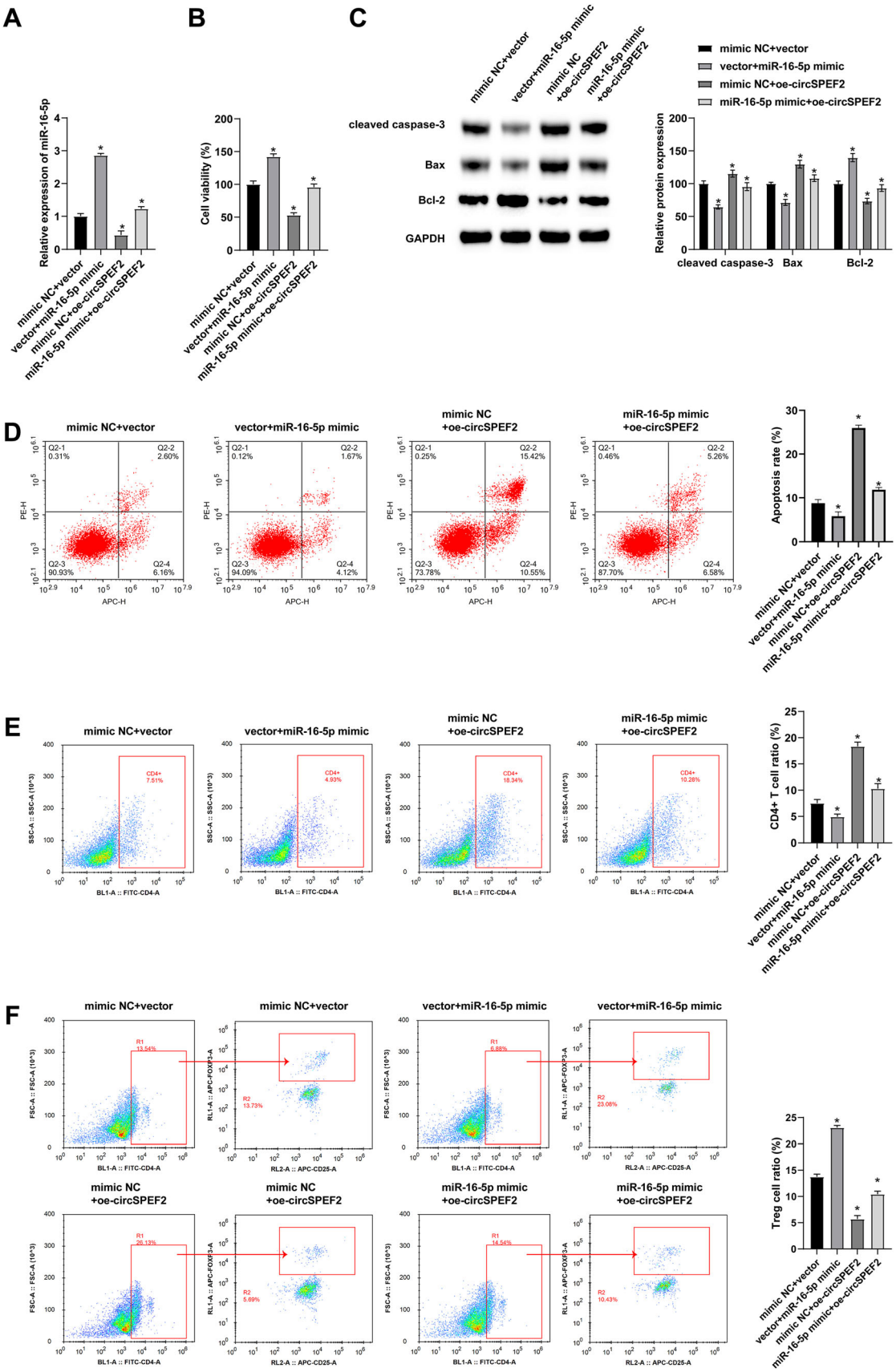
A
Relative expression of miR-16-5p
mimic NC+vector
vector+miR-16-5p mimic
mimic NC+oe-circSPEF2
miR-16-5p mimic+oe-circSPEF2
B
Cell viability (%)
C
cleaved caspase-3
Bax
Bcl-2
GAPDH
Relative protein expression
D
Apoptosis rate (%)
E
CD4+ T cell ratio (%)
F
Treg cell ratio (%)

◀**Fig. 4** circSPEF2 inhibits the malignant progression of DLBCL through miR-16-5p. After co-transfection of miR-16-5p mimic and oe-circSPEF2 into SU-DHL4 cells, **A** RT-qPCR checked miR-16-5p expression; **B** MTT assay analyzed the viability of SU-DHL4 cells; **C** Western blot measured apoptosis-related proteins; **D** Flow cytometry determined the apoptosis rate of SU-DHL4 cells in the co-culture system; **E–G** Flow cytometry detected the proportion of $CD4.^{+}$ and Treg cells in the co-culture system. Data were expressed as mean ± SD (N = 3). $p < 0.05$

2.13 Dual luciferase reporter assay

In starbase3.0 database (https://starbase.sysu.edu.cn/), the binding sites of miR-16-5p with circSPEF2 and BACH2 were predicted. The wild and mutant 3 'untranslated region sequences of circSPEF2 and BACH2 were inserted into the pmirGLO vector (Promega, Madison, WI, USA) to construct WT-circSPEF2, MUT-circSPEF2, WT-BACH2 and MUT-BACH2. The above plasmids and miR-16-5p mimic or mimic NC were transfected into SU-DHL-4 cells using Lipofectamine 3000 (Invitrogen). Luciferase activity was then assessed 48 h later using a dual luciferase reporter assay kit (Promega) and detected with Synergy 2 Multidetector Microplate Reader (BioTek Instruments Inc., Winooski, VT, USA).

2.14 Xenotransplantation in nude mice

All animal experiments were reviewed and approved by Huazhong University of Science and Technology Tongji Medical College Affiliated Union Hospital Animal Protection and Use Committee (Approval number: C2016TJ1128). Twenty 8-week-old male BALB/C nude mice (Shanghai Laboratory Animal Center of Chinese Academy of Sciences, Shanghai, China) were randomly divided into 4 groups: sh-NC + vector, sh-NC + oe-circSPEF2, sh-BACH2 + vector, sh-BACH2 + oe-circSPEF2. After anesthesia, 1×10^7 DLBCL cells transfected with the corresponding plasmid and lentivirus were injected subcutaneously into the right rib. The condition of nude mice and tumor growth were monitored daily, and tumor volume was recorded weekly for 4 weeks. Lymphoma tissues were collected from each euthanized mouse. The tumor volume was calculated as $0.5 \times \text{Width}^2 \times \text{Length}$.

2.15 Histological analysis

Lymphoma tissue was fixed with 4% paraformaldehyde for 4 h. After paraffin embedding, 5 μm thick sections were obtained using a microtome (RM2235, Leica, Wetzlar, Germany) and dried. For immunohistochemical staining, dewaxed slices were incubated overnight at 4 °C with Ki-67 antibody (1:100, Dako, Glostrup, Denmark) and incubated with HRP conjugated secondary antibody (1:3000; Dako) for 2 h. Finally, the slices were sealed with a quencher (Invitrogen) containing DAPI, and imaging analysis was performed using confocal microscopy. TUNEL staining was conducted using the commercial kit (Beyotime). Briefly, lymphoma tissue slices were incubated with a 50 μl TUNEL reaction mixture (45 μl labeled buffer and 5 μl TdT enzyme solution) at 37 °C for 60 min in darkness, dyed with DAPI solution at room temperature for 5 min, and imaged by fluorescence microscope (Olympus, Tokyo, Japan) and ImageJ software, respectively.

2.16 Data analysis

All data were analyzed and plotted using Graphpad 8.0. The data were expressed as mean ± standard deviation (SD). Student's *t*-test evaluated differences between the two groups, and one-way ANOVA evaluated those among multiple comparisons. At least three times replicates were required for each experiment. * $p < 0.05$ indicated statistical significance.

3 Results

3.1 circSPEF2 is decreased in DLBCL

circSPEF2 expression levels were checked in tissue samples from DLBCL patients, demonstrating a decreasing trend compared with healthy controls (Fig. 1A). circSPEF2 expression in DLBCL cell lines (SU-DHL4 and U2932) and GM12878 was also measured, and the results were consistent with those previously reported (Fig. 1B). The structure diagram of circSPEF2 is shown in Fig. 1C, which is located on SPEF2 gene of chromosome 5, with a length of about 557 bp. The stability of circSPEF2 was tested by RNAse R and actinomycin D. The structure shows that circSPEF2 presented resistance to the digestion of RNAse R and had a longer half-life than linear RNA (Fig. 1D, E). Meanwhile, circSPEF2 was mainly distributed in the cytoplasm (Fig. 1F).

3.2 Induction of circSPEF2 obstructs lymphoma cell proliferation and enhances immune response

To investigate the function of circSPEF2 in DLBCL, oe-circSPEF2 was transfected into SU-DHL4 cells to interfere with circSPEF2 expression. Figure 2A shows the increase in circSPEF2 expression. Subsequently, MTT assay

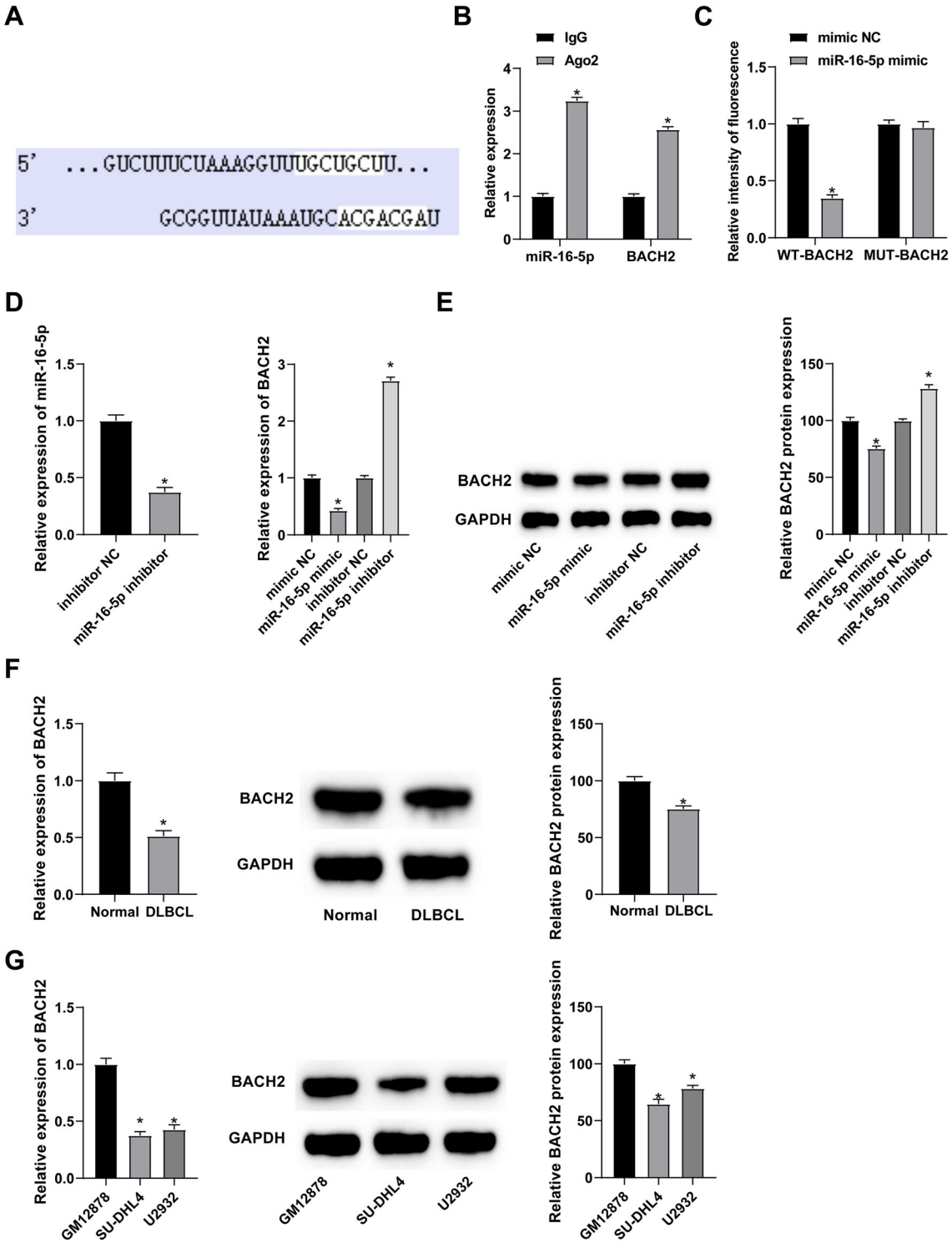

Fig. 5 BACH2 is mediated by miR-16-5p. **A** Map of potential binding sites of miR-16-5p and BACH2; **B** Ago2 enrichment level of miR-16-5p and BACH2 in SU-DHL4 cells; **C** Dual luciferase reporter assay verified the relationship between miR-16-5p and BACH2; **D**, **E** RT-qPCR and Western Blot measured miR-16-5p BACH2 after interference with miR-16-5p; **F**, **G** RT-qPCR and Western Blot measured BACH2 in tissues of DLBCL patients and cell lines. Data were expressed as mean ± SD (N = 3). $p < 0.05$

analyzed the viability of lymphoma SU-DHL4 cells and determined that elevating circSPEF2 obstructed the proliferative activity of SU-DHL4 cells (Fig. 2B). Changes in apoptosis-related proteins in SU-DHL4 cells were monitored. The outcomes indicated that enhancing circSPEF2 effectively increased Bax and Caspase-3 and decreased Bcl-2 protein expressions (Fig. 2C). At the same time, circSPEF2-overexpressed SU-DHL4 cells were co-cultured with activated T cells. Flow cytometry discovered that circSPEF2 overexpression could effectively increase the apoptosis rate of SU-DHL4 cells, expanded the proportion of $CD4^+$ cells in the co-culture system and compressed the proportion of Treg cells (Fig. 2D–G).

3.3 circSPEF2 targets miR-16-5p

To elucidate the mechanism of action of circSPEF2 in DLBCL, starbase 3.0 database offered the potential binding sites shared by circSPEF2 and miR-16-5p (Fig. 3A). The enrichment of circSPEF2 and miR-16-5p in Ago2 magnetic beads was verified by RIP experiment (Fig. 3B). miR-16-5p mimic was transfected into DLBCL cells, resulting in the upregulation of miR-16-5p (Fig. 3C). Dual luciferase assay confirmed the circSPEF2 targeting regulation of miR-16-5p. When co-transfected miR-16-5p mimic with WT-circSPEF2 reporter gene, luciferase activity decreased significantly. However, no significant changes occurred when co-transfected miR-16-5p mimic and mu-circSPEF2 reporter gene (Fig. 3D). RT-qPCR analyzed that circSPEF2 overexpression reduced miR-16-5p expressions (Fig. 3E). Meanwhile, miR-16-5p was upregulated in tissues of DLBCL patients and tumor cell lines (Fig. 3F, G).

3.4 ircSPEF2 inhibits the malignant progression of DLBCL through miR-16-5p

To further explore the mechanism of circSPEF2 and miR-16-5p in DLBCL, a functional salvage experiment was conducted. First, miR-16-5p mimic and oe-circSPEF2 were co-transfected into SU-DHL4 cells. The results of RT-qPCR test showed that miR-16-5p mimic reversibly elevated miR-16-5p expression in cells previously interfered with oe-circSPEF2 (Fig. 4A). MTT assay results discovered that circSPEF2 overexpression inhibited the proliferation of SU-DHL4 cells, upregulating miR-16-5p mitigated this inhibition (Fig. 4B). Meanwhile, Western Blot analysis also confirmed that inducing miR-16-5p could inactivate the apoptotic activity of SU-DHL4 cells (Fig. 4C). Co-transfected SU-DHL4 cells were then co-cultured with activated T cells, and flow cytometry results revealed that the promotion effect of circSPEF2 on SU-DHL4 apoptosis rate, $CD4^+$ immune cell proportion and inhibition effect on Treg cell proportion were reversible upon miR-16-5p overexpression (Fig. 4D–G).

3.5 BACH2 is the downstream target of miR-16-5p

According to the function of miRNA, the current work searched for downstream targets of miR-16-5p through starbase 3.0. Figure 5A presents potential binding sites between miR-16-5p and BACH2. At the same time, RIP experiment detected the enrichment of miR-16-5p and BACH2 in Ago2 magnetic beads (Fig. 5B). To confirm BACH2 as the direct target of miR-16-5p, dual luciferase reporter assay was performed, showing the inhibition of luciferase activity in miR-16-5p mimic + WT-BACH2-co-transfected SU-DHL4 cells (Fig. 5C). Moreover, overexpressing miR-16-5p could lower BACH2 expressions, while silencing of miR-16-5p had the opposite result (Fig. 5D, E). RT-qPCR and Western Blot detected downregulated BACH2 expression in DLBCL patients and cell lines (Fig. 5F, G).

3.6 circSPEF2 delays the malignant progression of DLBCL through the miR-16-5p/BACH2 axis

To study the role of circSPEF2/miR-16-5p/BACH axis in DLBCL, si-BACH2 and oe-circSPEF2 were co-transfected into DLBCL cells, and si-BACH2 contributed to the reversible downregulation of BACH2 in circSPEF2-overexpressed SU-DHL4 cells (Fig. 6A). In MTT rescue experiment, BACH2 knockdown led to a proliferation reversal in circSPEF2-overexpressed SU-DHL4 cells (Fig. 6B). Western Blot results showed that depleting BACH2 could also reversibly reduce the promoting effect of circSPEF2 on SU-DHL4 apoptosis (Fig. 6C). Meanwhile, flow cytometry also confirmed the reversible effect of silenced BACH2 on immune escape in the co-culture system (Fig. 6D–G).

3.7 circSPEF2 suppresses DLBCL tumor growth and immune escape

Finally, the molecular mechanism of circSPEF2 in DLBCL progression was studied using BALB/C nude mice. SU-DHL4 cells or SU-DHL4 cells transfected with sh-BACH2 and oe-circSPEF2 were implanted into the right rib of nude mice. Anatomical results showed that tumor growth was significant in mice implanted with negative control, and silencing BACH2 re-promoted tumor growth based on overexpression of circSPEF2 (Fig. 7A-C). Western Blot results showed that knockdown of BACH2 could suppress the promoting effect of circSPEF2 overexpression on BACH2 expression *in vivo* (Fig. 7D). Subsequently, IHC results tested that overexpressing circSPEF2 reduced Ki-67

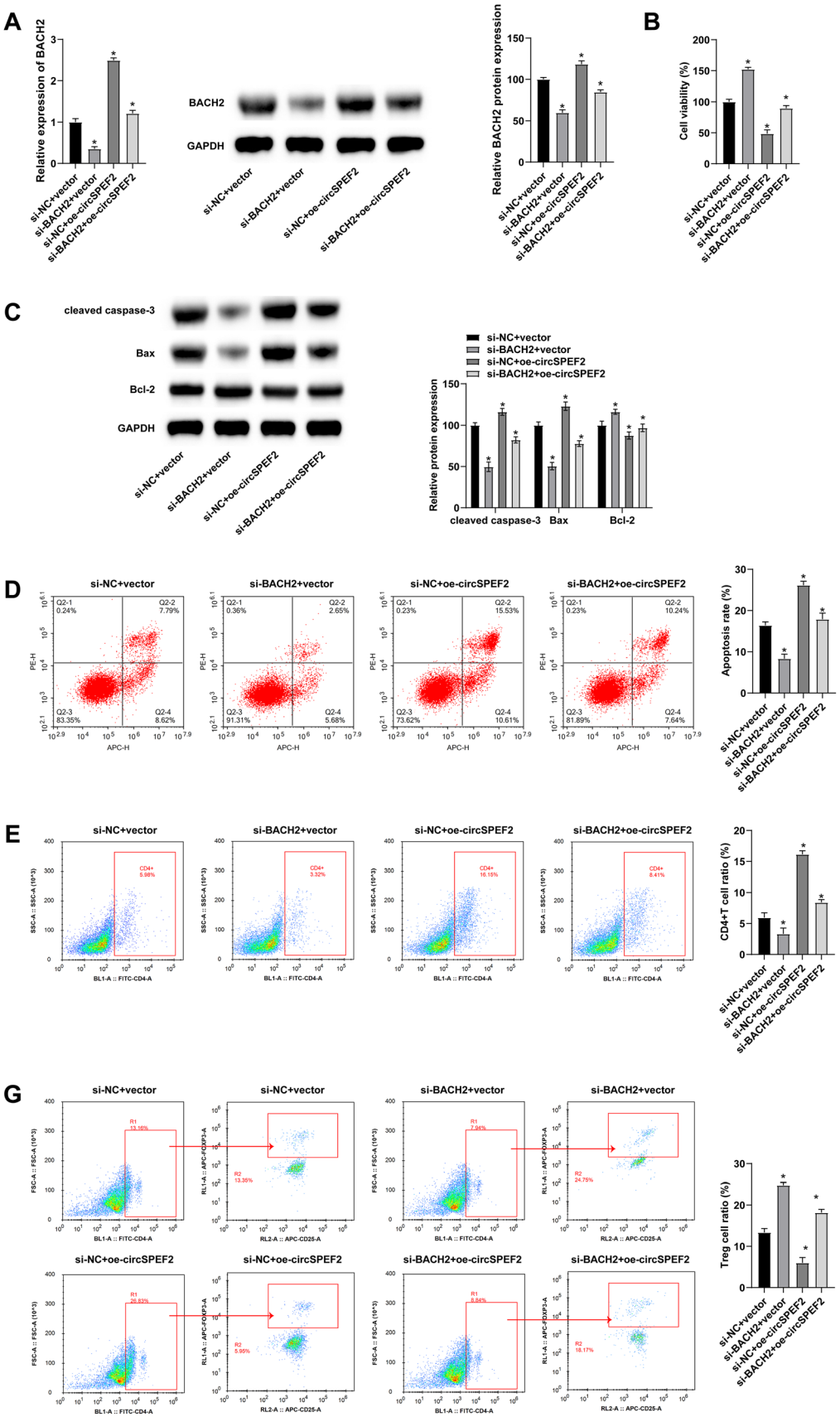
A
Relative expression of BACH2
si-NC+vector
si-BACH2+vector
si-NC+oe-circSPEF2
si-BACH2+oe-circSPEF2
BACH2
GAPDH
Relative BACH2 protein expression
B
Cell viability (%)
C
cleaved caspase-3
Bax
Bcl-2
GAPDH
Relative protein expression
D
Apoptosis rate (%)
E
CD4+T cell ratio (%)
G
Treg cell ratio (%)

◀**Fig. 6** circSPEF2 inhibits malignant progression of DLBCL through the miR-16-5p/BACH2 axis. si-BACH2 and oe-circSPEF2 were co-transfected into DLBCL cells, **A** RT-qPCR and Western Blot measured BACH2 expression; **B** MTT assay analyzed the viability of SU-DHL4 cells; **C** Western blot measured apoptosis-related proteins; **D** Flow cytometry determined the apoptosis rate of SU-DHL4 cells in the co-culture system; **E–G** Flow cytometry detected the proportion of $CD4.^{+}$ and Treg cells in the co-culture system. Data were expressed as mean ± SD (N = 3). $p < 0.05$

signaling in tumors, while knockdown of BACH2 reversed this reduction (Fig. 7E). TUNEL staining was performed on the slices to analyze the apoptosis of tumor cells. The results showed that the number of positive cells in the tumor of mice overexpressed with circSPEF2 was increased, but this number was reduced by depleting BACH2 (Fig. 7F). Meanwhile, Western Blot test results elucidated that BACH2 downregulation following circSPEF2 overexpression had a reversible effect on apoptotic proteins (Fig. 8A) and on apoptosis of lymphoma cells and immune escape (Fig. 8B–D).

4 Discussion

As the most common subtype of NHL, DLBCL has a poor prognosis and limited therapeutic effectiveness [32]. circRNA indicates significance in tumorigenesis and tumor progression [33]. Based on this, the current work focused on circSPEF2 and explained the mechanism of circSPEF2 in DLBCL. In short, circSPEF2 could inhibit the growth

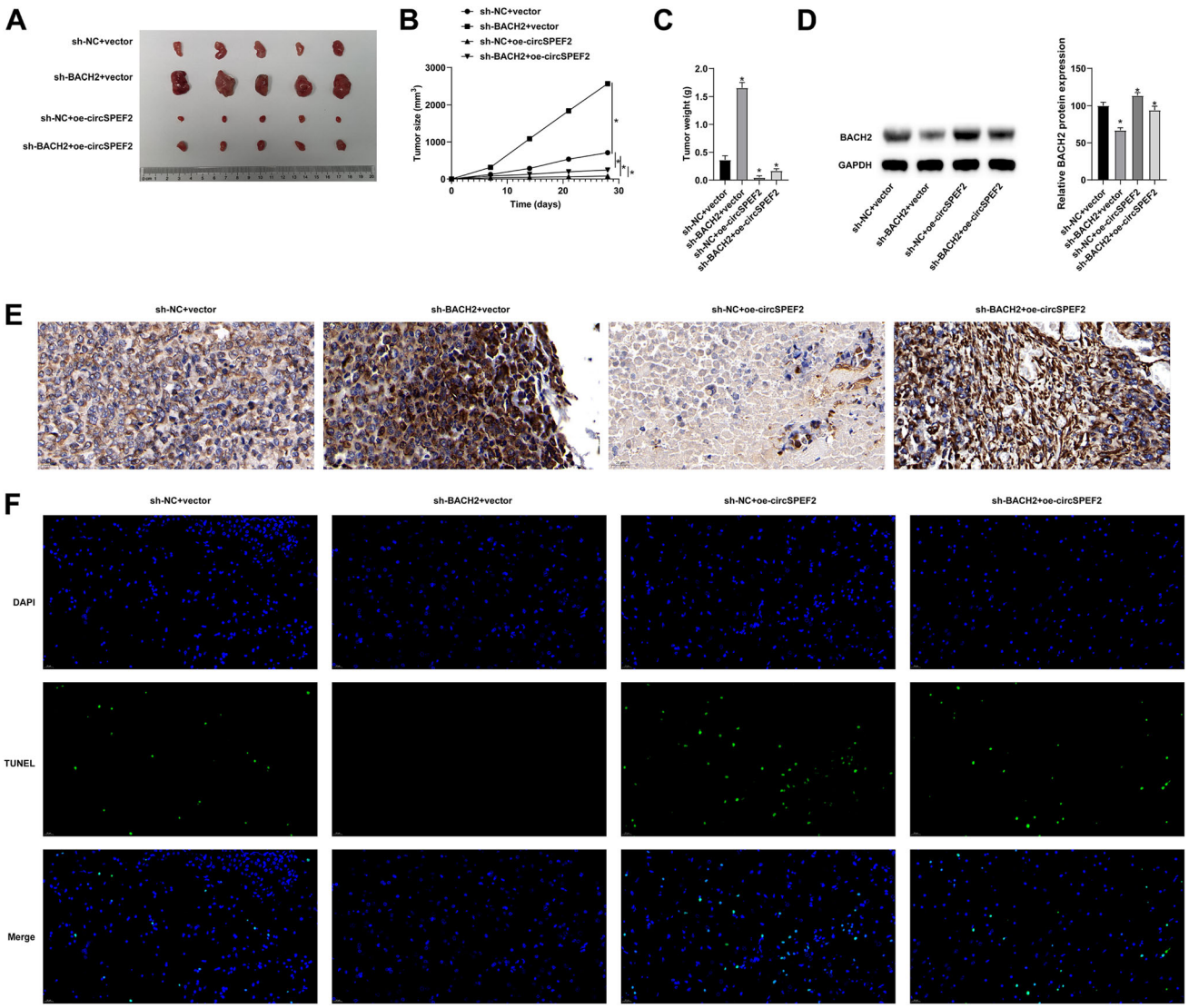

Fig. 7 circSPEF2 suppresses DLBCL tumor growth and immune escape. **A** Representative tumor images in each group (5/group); **B** tumor growth curve; **C** tumor volume; **D** Western Blot checked BACH2; **E** IHC staining observed Ki-67 signal; **F** TUNEL staining detected apoptosis of tumor cells; Data were expressed as mean ± SD (N = 3). $P < 0.05$

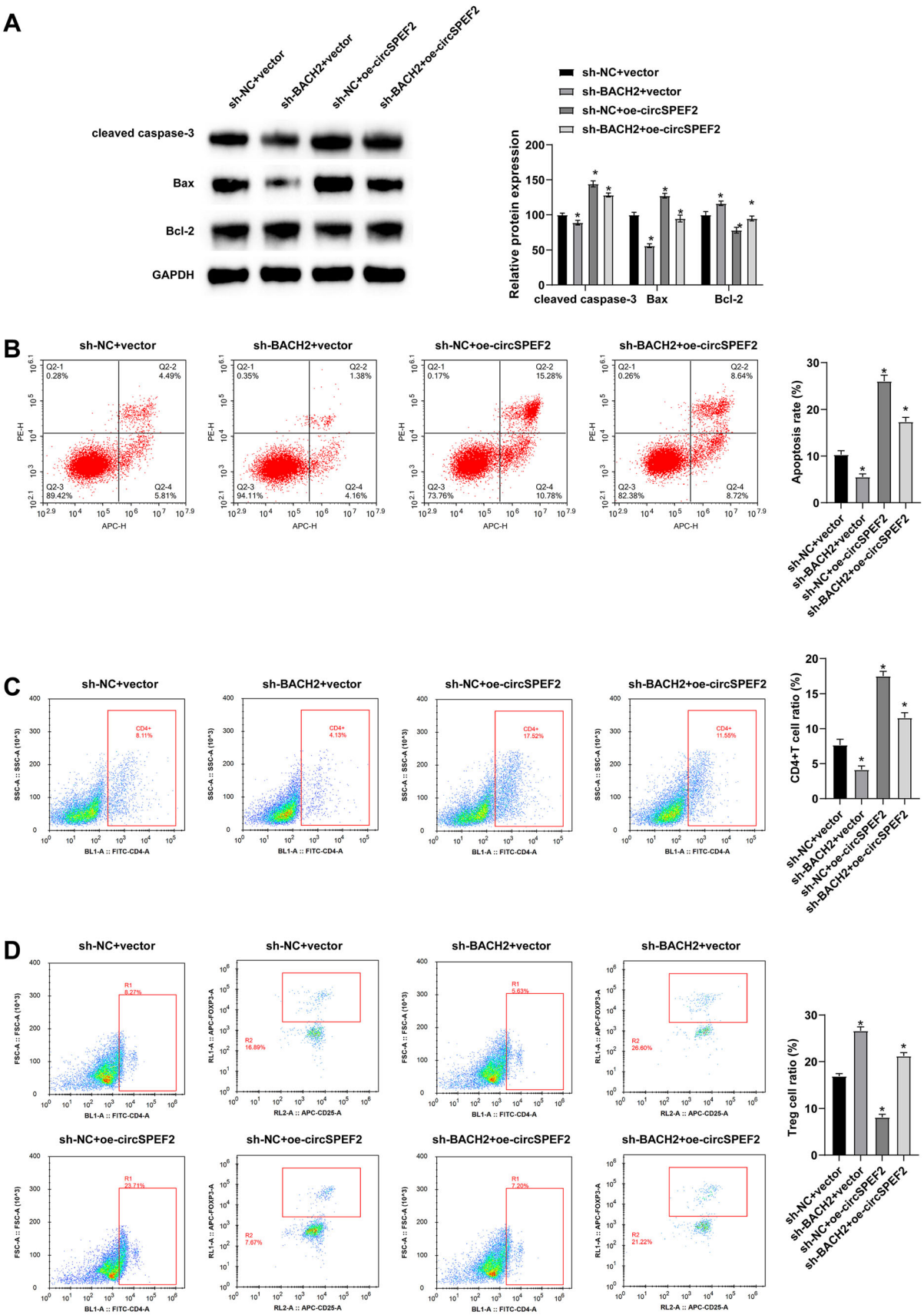
A
sh-NC+vector
sh-BACH2+vector
sh-NC+oe-circSPEF2
sh-BACH2+oe-circSPEF2
cleaved caspase-3
Bax
Bcl-2
GAPDH
Relative protein expression
cleaved caspase-3
Bax
Bcl-2
B
Q2-1 0.28%
Q2-2 4.49%
Q2-3 89.42%
Q2-4 5.81%
Q2-1 0.35%
Q2-2 1.38%
Q2-3 94.11%
Q2-4 4.16%
Q2-1 0.17%
Q2-2 15.28%
Q2-3 73.76%
Q2-4 10.78%
Q2-1 0.26%
Q2-2 8.64%
Q2-3 82.38%
Q2-4 8.72%
PE-H
APC-H
Apoptosis rate (%)
C
CD4+ 8.11%
CD4+ 4.13%
CD4+ 17.52%
CD4+ 11.55%
SSC-A :: SSC-A (10^3)
BL1-A :: FITC-CD4-A
CD4+T cell ratio (%)
D
R1 8.27%
R2 16.89%
R1 5.63%
R2 26.60%
R1 23.71%
R2 7.67%
R1 7.20%
R2 21.22%
FSC-A :: FSC-A (10^3)
RL1-A :: APC-FOXP3-A
RL2-A :: APC-CD25-A
Treg cell ratio (%)

◀**Fig. 8** circSPEF2 suppresses DLBCL tumor growth and immune escape. **A** Western blot measured apoptosis-related proteins; **B–D** Flow cytometry measured apoptosis and immune cell $CD4.^{+}$ to Treg ratio in lymphoma. Data were expressed as mean ± SD (N = 3). $P < 0.05$

and immune escape of DLBCL cells via the miR-16-5p/BACH2 axis.

Malregulated circRNAs are associated with cancer development [12, 34, 35]. Therefore, elucidating the function of circRNA in DLBCL is conducive to the development of new therapeutic methods. A recent study analyzes that circEAF2 is downregulated in DLBCL and negatively correlated with DLBCL progression in EBV infection [17]. Meanwhile, sequencing data found that hsa_circ_012889 is also downregulated in EBV-infected DLBCL, and hsa_circ_012889 (circSPEF2) is a newly discovered circRNA that has not yet been studied. Therefore, this study detected circSPEF2 expression in DLBCL patients and cell lines, and the results were consistent with our conjectures. Subsequently, it was proved that circSPEF2 inhibited proliferative activity of DLBCL cells, and elevated apoptosis of cancer cells and the expression of apoptosis-related proteins Bax and Caspase-3. It is worth mentioning that the immune system is a key role in tumor progression, and suppressing the immune escape of tumors is the core concept of cancer immunotherapy. Tregs cells are present in tumor areas of most cancers and contribute to the immune escape [36–38]. BACH2 promoted tumor immunosuppression through Treg-mediated inhibition of intratumoral $CD8^{+}$ T cells and IFN-γ, and induce long-term non-response or apoptosis of $CD4^{+}$ and $CD8^{+}$T cells [39, 40]. This study, however, demonstrated novelly that circSPEF2 increased the proportion of CD4 T cells and decreased the proportion of Treg cells in the co-culture system, suggesting that circSPEF2 is a potential therapeutic target by inhibiting proliferation and promoting apoptosis, as well as enhancing the anti-tumor immune response.

miRNA can be regulated by circRNA to affect tumor progression. This mechanism is also present in the development of DLBCL [16, 41, 42]. However, a recent study has demonstrated that DLBCL cells secrete more exosomes than normal cells, including miR-16-5p [43]. miR-16-5p is considered to be a carcinogenic factor in hepatocellular carcinoma [44] and ovarian cancer [45]. This study revealed the involvement of miR-16-5p in DLBCL progression due to its abnormal upregulation trend. Moreover, miR-16-5p was the downstream target of circSPEF2, and induction of miR-16-5p abolished the effect of circSPEF2 on the growth of DLBCL cells and the promotion of apoptosis. miR-16-5p has been reported to influence the number of Treg populations in the breast cancer microenvironment [26]. This work found that miR-16-5p inhibited the amount of CD4 and increased the proportion of Treg cells in the co-culture system, confirming that circSPEF2 can participate in the malignant progression and immune escape of DLBCL through the regulation of miR-16-5p.

Next, miR-16-5p has a targeting relationship with BACH2. This is similar to the study by Liu et al. [46]. A late paper confirms that overall survival in chronic lymphocytic leukemia is lower in patients with low BACH2 levels [47]. BACH2 is a potential T-cell lymphoma tumor suppressor, in the absence of Bach2, CD4 (+) T cells demonstrate an augmented propensity towards effector cell differentiation, resulting in elevated production of Th2-related cytokines and a diminished generation of regulatory T cells [48]. A recent study shows that patients with higher BACH2 expression in DLBCL had a better prognosis [49]. The potential involvement of circSPEF2 in the regulation of other host genes cannot be disregarded. However, our study specifically verified the interaction between circSPEF2 and mir-16-5p, and further proved that silencing BACH2 could reverse the influence of circSPEF2 overexpression on DLBCL cell proliferation, apoptosis, and immune response in TME. Meanwhile, influences of circSPEF2 on tumor growth and immune response were abolished by depleting BACH2. Current research is not clear whether circSPEF2 inhibits DLBCL cells by targeting downstream genes of the miR-16-5p/BACH2 axis, which may have a synergistic effect with this study's mechanisms, necessitating additional research to substantiate this claim.

Although we did not investigate the conservative relationship of the circSPEF2/miR-16-5p/BACH2 axis in a wider range of DLBCL cell lines, our animal studies demonstrated that silencing BACH2 reversed the inhibitory effect of circSPEF2 overexpression on tumor growth, thereby promoting tumor growth. In future studies, we intend to explore the conservative relationship of the circSPEF2/miR-16-5p/BACH2 axis in different DLBCL cell lines.This work has not yet investigated the relationship between circSPEF2 expression levels and DLBCL progression and its relationship to the prognosis of DLBCL patients. Secondly, this work has not yet explored the detailed molecular mechanism of how circSPEF2 influences apoptosis of DLBCL cells and changes in immune homeostasis in the TME by mediating the miR-16-5p/BACH2 axis. Moreover, studies should further look for other potential modes of circSPEF2 in different DLBCL cell lines, with a view to providing new strategies for the treatment of DLBCL patients.

In conclusion, circSPEF2 can affect the proliferation and apoptosis of DLBCL cells and the balance of Treg and CD4 immune cells in the TME through the miR-16-5p/BACH2 axis, and inhibit the malignant progression of DLBCL.

Acknowledgements Not applicable.

Author contributions JZ designed the research study. MX and ZC performed the research. LH and ZW provided help and advice. ZH, LL and JZ analyzed the data. JZ wrote the manuscript. LL reviewed and edited the manuscript. All authors contributed to editorial changes in the manuscript. All authors read and approved the final manuscript.

Data availability statement The datasets used and/or analyzed during the present study are available from the corresponding author on reasonable request.

Declarations

Conflict of interest The authors have no conflicts of interest to declare.

Ethical statement The present study was approved by the Ethics Committee of Huazhong University of Science and Technology Tongji Medical College Affiliated Union Hospital and written informed consent was provided by all patients prior to the study start (Approval number: C2016TJ1117). All procedures were performed in accordance with the ethical standards of the Institutional Review Board and The Declaration of Helsinki, and its later amendments or comparable ethical standards.
All animal experiments were reviewed and approved by Huazhong University of Science and Technology Tongji Medical College Affiliated Union Hospital Animal Protection and Use Committee (Approval number: C2016TJ1128).

References

1. Sehn LH, Gascoyne RD. Diffuse large B-cell lymphoma: optimizing outcome in the context of clinical and biologic heterogeneity. Blood. 2015;125:22–32.
2. Yin X, Xu A, Fan F, Huang Z, Cheng Q, Zhang L, et al. Incidence and mortality trends and risk prediction nomogram for extranodal diffuse large B-cell lymphoma: an analysis of the surveillance, epidemiology, and end results database. Front Oncol. 2019;9:1198.
3. Jiang X, Wang J, Deng X, Xiong F, Ge J, Xiang B, et al. Role of the tumor microenvironment in PD-L1/PD-1-mediated tumor immune escape. Mol Cancer. 2019;18:10.
4. Eichmüller SB, Osen W, Mandelboim O, Seliger B. Immune modulatory microRNAs involved in tumor attack and tumor immune escape. J Natl Cancer Inst. 2017. https://doi.org/10.1093/jnci/djx034
5. Laurent C, Charmpi K, Gravelle P, Tosolini M, Franchet C, Ysebaert L, et al. Several immune escape patterns in non-Hodgkin's lymphomas. Oncoimmunology. 2015;4:e1026530.
6. Zou W. Regulatory T cells, tumour immunity and immunotherapy. Nat Rev Immunol. 2006;6:295–307.
7. Afshar-Sterle S, Zotos D, Bernard NJ, Scherger AK, Rödling L, Alsop AE, et al. Fas ligand-mediated immune surveillance by T cells is essential for the control of spontaneous B cell lymphomas. Nat Med. 2014;20:283–90.
8. Strasser A, Jost PJ, Nagata S. The many roles of FAS receptor signaling in the immune system. Immunity. 2009;30:180–92.
9. Kelley TW, Parker CJ. CD4 (+)CD25 (+)Foxp3 (+) regulatory T cells and hematologic malignancies. Front Biosci (Schol Ed). 2010;2:980–92.
10. Strauss L, Bergmann C, Whiteside TL. Human circulating CD4+CD25highFoxp3+ regulatory T cells kill autologous CD8+ but not CD4+ responder cells by Fas-mediated apoptosis. J Immunol. 2009;182:1469–80.
11. Mahnke K, Bedke T, Enk AH. Regulatory conversation between antigen presenting cells and regulatory T cells enhance immune suppression. Cell Immunol. 2007;250:1–13.
12. Kristensen LS, Jakobsen T, Hager H, Kjems J. The emerging roles of circRNAs in cancer and oncology. Nat Rev Clin Oncol. 2022;19:188–206.
13. Shi Y, Ding D, Qu R, Tang Y, Hao S. Non-coding RNAs in diffuse large B-cell lymphoma. Onco Targets Ther. 2020;13:12097–112.
14. Deng L, Liu G, Zheng C, Zhang L, Kang Y, Yang F. Circ-LAMP1 promotes T-cell lymphoblastic lymphoma progression via acting as a ceRNA for miR-615-5p to regulate DDR2 expression. Gene. 2019;701:146–51.
15. Perez de Acha O, Rossi M, Gorospe M. Circular RNAs in blood malignancies. Front Mol Biosci. 2020;7:109.
16. Lin D, Wang Y, Lei L, Lin C. Circ_0003645 serves as miR-335-5p sponge to promote the biological process of diffuse large B-cell lymphoma by upregulating NFIB. Autoimmunity. 2022;55:127–35.
17. Zhao CX, Yan ZX, Wen JJ, Fu D, Xu PP, Wang L, et al. Circ-cEAF2 counteracts Epstein-Barr virus-positive diffuse large B-cell lymphoma progression via miR-BART19-3p/APC/beta-catenin axis. Mol Cancer. 2021;20:153.
18. Cen J, Liang Y, Huang Y, Pan Y, Shu G, Zheng Z, et al. Circular RNA circSDHC serves as a sponge for miR-127-3p to promote the proliferation and metastasis of renal cell carcinoma via the CDKN3/E2F1 axis. Mol Cancer. 2021;20:19.
19. Wang L, Yang B, Xu Z, Song X, Gong Z, Xue S, et al. NRF1-regulated CircNSUN2 promotes lymphoma progression through activating Wnt signaling pathway via stabilizing HMGA1. Cell Cycle. 2021;20:819–28.
20. Bartel DP. MicroRNAs: genomics, biogenesis, mechanism, and function. Cell. 2004;116:281–97.
21. Tagawa H, Ikeda S, Sawada K. Role of microRNA in the pathogenesis of malignant lymphoma. Cancer Sci. 2013;104:801–9.
22. Yan S, Chen Y, Yang M, Zhang Q, Ma J, Liu B, et al. hsa-MicroRNA-28-5p inhibits diffuse large B-cell lymphoma cell proliferation by downregulating 14-3-3zeta expression. Evid Based Complement Alternat Med. 2022;2022:4605329.
23. Yu CY, Kuo HC. The emerging roles and functions of circular RNAs and their generation. J Biomed Sci. 2019;26:29.
24. Hu H, Chen C, Chen F, Sun N. LINC00152 knockdown suppresses tumorigenesis in non-small cell lung cancer via sponging miR-16-5p. J Thorac Dis. 2022;14:614–24.
25. Lou J, Zhang H, Xu J, Ren T, Huang Y, Tang X, et al. circUSP34 accelerates osteosarcoma malignant progression by sponging miR-16-5p. Cancer Sci. 2022;113:120–31.
26. Ni C, Fang QQ, Chen WZ, Jiang JX, Jiang Z, Ye J, et al. Breast cancer-derived exosomes transmit lncRNA SNHG16 to induce CD73+gammadelta1 Treg cells. Signal Transduct Target Ther. 2020;5:41.
27. Zhou Y, Wu H, Zhao M, Chang C, Lu Q. The bach family of transcription factors: A comprehensive review. Clin Rev Allergy Immunol. 2016;50:345–56.
28. Yang L, Chen S, Zhao Q, Sun Y, Nie H. The critical role of Bach2 in shaping the balance between CD4(+) T cell subsets in

immune-mediated diseases. Mediat Inflamm. 2019;2019:2609737.
29. Roychoudhuri R, Hirahara K, Mousavi K, Clever D, Klebanoff CA, Bonelli M, et al. BACH2 represses effector programs to stabilize T(reg)-mediated immune homeostasis. Nature. 2013;498:506–10.
30. Kuwahara M, Ise W, Ochi M, Suzuki J, Kometani K, Maruyama S, et al. Bach2-Batf interactions control Th2-type immune response by regulating the IL-4 amplification loop. Nat Commun. 2016;7:12596.
31. Chen Y, Li M, Cao J, Cai G, Li X, Liu Y, et al. CTLA-4 promotes lymphoma progression through tumor stem cell enrichment and immunosuppression. Open Life Sci. 2021;16:909–19.
32. Rovira J, Valera A, Colomo L, Setoain X, Rodríguez S, Martínez-Trillos A, et al. Prognosis of patients with diffuse large B cell lymphoma not reaching complete response or relapsing after frontline chemotherapy or immunochemotherapy. Ann Hematol. 2015;94:803–12.
33. Arnaiz E, Sole C, Manterola L, Iparraguirre L, Otaegui D, Lawrie CH. CircRNAs and cancer: biomarkers and master regulators. Semin Cancer Biol. 2019;58:90–9.
34. Huang G, Liang M, Liu H, Huang J, Li P, Wang C, et al. CircRNA hsa_circRNA_104348 promotes hepatocellular carcinoma progression through modulating miR-187-3p/RTKN2 axis and activating Wnt/beta-catenin pathway. Cell Death Dis. 2020;11:1065.
35. Liu Z, Zhou Y, Liang G, Ling Y, Tan W, Tan L, et al. Circular RNA hsa_circ_001783 regulates breast cancer progression via sponging miR-200c-3p. Cell Death Dis. 2019;10:55.
36. Elkoshi Z. "High Treg" inflammations promote (most) non-hematologic cancers while "Low Treg" inflammations promote lymphoid cancers. J Inflamm Res. 2020;13:209–21.
37. Mittal S, Marshall NA, Duncan L, Culligan DJ, Barker RN, Vickers MA. Local and systemic induction of CD4+CD25+ regulatory T-cell population by non-Hodgkin lymphoma. Blood. 2008;111:5359–70.
38. Shang B, Liu Y, Jiang SJ, Liu Y. Prognostic value of tumor-infiltrating FoxP3+ regulatory T cells in cancers: a systematic review and meta-analysis. Sci Rep. 2015;5:15179.
39. Zhao DM, Thornton AM, DiPaolo RJ, Shevach EM. Activated CD4+CD25+ T cells selectively kill B lymphocytes. Blood. 2006;107:3925–32.
40. Pandiyan P, Zheng L, Ishihara S, Reed J, Lenardo MJ. CD4+CD25+Foxp3+ regulatory T cells induce cytokine deprivation-mediated apoptosis of effector CD4+ T cells. Nat Immunol. 2007;8:1353–62.
41. Hu Y, Zhao Y, Shi C, Ren P, Wei B, Guo Y, et al. A circular RNA from APC inhibits the proliferation of diffuse large B-cell lymphoma by inactivating Wnt/beta-catenin signaling via interacting with TET1 and miR-888. Aging (Albany NY). 2019;11:8068–84.
42. Liu W, Lei L, Liu X, Ye S. CircRNA_OTUD7A upregulates FOXP1 expression to facilitate the progression of diffuse large B-cell lymphoma via acting as a sponge of miR-431-5p. Genes Genom. 2021;43:653–67.
43. Moloudizargari M, Hekmatirad S, Mofarahe ZS, Asghari MH. et al. Exosomal microRNA panels as biomarkers for hematological malignancies. Curr Probl Cancer. 2021;45:100726.
44. Peng R, Cao J, Su BB, Bai XS, Jin X, Wang AQ, et al. Down-regulation of circPTTG1IP induces hepatocellular carcinoma development via miR-16-5p/RNF125/JAK1 axis. Cancer Lett. 2022;543:215778.
45. Saral MA, Tuncer SB, Odemis DA, Erdogan OS, Erciyas SK, Saip P, et al. New biomarkers in peripheral blood of patients with ovarian cancer: high expression levels of miR-16-5p, miR-17-5p, and miR-638. Arch Gynecol Obstet. 2022;305:193–201.
46. Liu X, Su K, Kuang S, Fu M, Zhang Z. miR-16-5p and miR-145-5p trigger apoptosis in human gingival epithelial cells by down-regulating BACH2. Int J Clin Exp Pathol. 2020;13:901–11.
47. Ciardullo C, Szoltysek K, Zhou P, Pietrowska M, Marczak L, Willmore E, et al. Low BACH2 expression predicts adverse outcome in chronic lymphocytic leukaemia. Cancers (Basel). 2021;14:23.
48. Daniels J, Choi J. BACH2 is a putative T-cell lymphoma tumor suppressor that may play a role in product-derived CAR T-cell lymphomas. Blood. 2021;138:2731–3.
49. Kamio T, Toki T, Kanezaki R, Sasaki S, Tandai S, Terui K, et al. B-cell-specific transcription factor BACH2 modifies the cytotoxic effects of anticancer drugs. Blood. 2003;102:3317–22.